APPLIED AND ENVIRONMENTAL MICROBIOLOGY, Feb. 1977, p. 406-426
Vol. 33, No. 2

Printed in U.S.A.

In Situ Morphology of the Gut Microbiota of Wood-Eating Termites [*Reticulitermes flavipes* (Kollar) and *Coptotermes formosanus* Shiraki][1]

JOHN A. BREZNAK* AND H. STUART PANKRATZ

Department of Microbiology and Public Health, Michigan State University, East Lansing, Michigan 48824

Received for publication 13 July 1976

Light microscopy and scanning and transmission electron microscopy were used to examine the in situ morphology of the gut microbiota of *Reticulitermes flavipes* and *Coptotermes formosanus*. Laboratory-maintained termites were used and, for *R. flavipes*, specimens were also prepared immediately after collection from a natural infestation. The latter endeavor enabled a study of different castes and developmental stages of *R. flavipes* and revealed differences in the microbiota of field versus laboratory specimens. The termite paunch microbiota consisted of an abundance of morphologically diverse bacteria and protozoa. Thirteen bacterial morphotypes in the paunch were described in detail: seven were observed only in *R. flavipes*, three were observd only in *C. formosanus*, and three were common to both termite species. The paunch epithelium was densely colonized by bacteria, many of which possessed holdfast elements that secured them tightly to this tissue and to other bacterial cells. Besides bacteria, the protozoan *Pyrsonympha vertens* adhered to the paunch epithelium of *R. flavipes* by means of an attachment organelle. Cuplike indentations were present on the paunch epithelial surface and were sites of bacterial aggregation. Ultrastructural features of cups suggested their involvement in ion absorption. In addition to the paunch, the midgut was also colonized by bacteria that were situated between epithelial microvilli. Results suggest that bacteria are an integral part of the gut ecosystem.

A true mutualism exists between wood-eating termites and certain cellulolytic protozoa that reside in the insect's hindgut (13, 23, 27). It is unfortunate, however, that only fragmentary information exists regarding the bacterial component of the gut microbiota, particularly since the concentration of bacteria has been estimated to be 10^8 to 10^{10} cells/ml of hindgut fluid (13).

As part of an overall project designed to assess more fully the nature and roles of bacteria in the termite gut ecosystem, we employed a microscopy approach. Other workers have also used microscopy to examine termite gut bacteria (30, 31, 36). However, such efforts were largely secondary to a major emphasis on gut anatomy and physiology, and the microbiota was not described in detail. In the present study we employed light microscopy, scanning electron microscopy (SEM), and transmission electron microscopy (TEM) to pursue the following main goals: (i) to determine the morphological diversity of bacteria that colonize the gut; (ii) to determine whether the gut epithelium serves as a site for attachment of bacteria (a situation that might facilitate biochemical interaction between termites and bacteria); and (iii) to attempt to define, morphologically, bacteria that might constitute part of the autochthonous (40) flora of termites. Collaterally, because little work has been done on the cytology of the alimentary tract of *Rhinotermitidae* (the family to which the termites under study belong), we hoped to contribute to a better understanding of this aspect of termite biology.

(A preliminary report of portions of this work was presented as part of the 29th Symposium of the Society for Experimental Biology, 2-6 September 1974, Bristol, England [13], and at the 75th Annual Meeting of the American Society for Microbiology, 27 April-2 May 1975, New York, N.Y.)

MATERIALS AND METHODS

Termites. *C. formosanus* was collected near Lake Charles, La., whereas *R. flavipes* was collected in Janesville, Wis. Termite-infested wood, with adherent soil and debris from the collection site, was kept

[1] Journal article no. 7744 from the Michigan Agricultural Experiment Station.

at 24°C in galvanized trash containers. In addition, "wood packs," consisting of stacks of 20 1-cm slices of commercial Douglas fir lumber (2 by 6 inches [ca. 5.08 by 15.24 cm]), were thoroughly wetted with distilled water and added to containers of *C. formosanus*. For *R. flavipes*, 10-cm lengths of Douglas fir (2 by 6 inches) were placed vertically in trash containers on top of infested wood and covered with moistened white paper towels (singlefold, no. 211 Palmer Towels; Fort Howard Paper Co., Green Bay, Wis.). In this way, termites aggregated between wood slices or directly beneath paper towels, thereby facilitating their removal without disrupting the entire contents of containers.

For antibiotic treatment, termites were held at 24°C in 2-ounce (ca. 0.06-liter) screw-cap jars. Oven-dried Douglas fir sawdust, which had been previously extracted three times with boiling distilled water, was thoroughly wetted with a basal salts solution (14) containing (in micrograms per milliliter): tetracycline, 800; penicillin, 900; and chloramphenicol and streptomycin sulfate, 1,000 each. Excess fluid was removed by squeezing the material between the fingers, and a volume of about 2 cm^3 of moist sawdust was added to each jar.

The terminology used to indicate the developmental stage or caste of termites was that of Esenther (19) for *R. flavipes* and that of King and Spink (28) for *C. formosanus*.

Preparation of guts and microscopy. Hindguts were withdrawn from termites by using forceps (7). The withdrawn hindguts, usually with a segment of midgut attached (Fig. 1), were immediately placed in a drop of 2.5% glutaraldehyde in 0.1 M potassium phosphate buffer (pH 7.0) on a sheet of dental wax. The paunch region of the hindgut (Fig. 1) was sliced with a razor to allow rapid penetration of fixative into the paunch lumen. Gut segments were then transferred to vials containing fixative and kept at 5°C for several hours to overnight before washing three times with glutaraldehyde-free phosphate buffer.

In attempts to wash organisms out of the hindgut, guts were removed and sliced as above, but in a drop of phosphate buffer containing 0.85% NaCl. Gut segments were then transferred to a vial containing 5 ml of the same solution and agitated gently by hand or vigorously for 60 s with the aid of a Vortex mixing device. Segments were allowed to settle and, after aspiration of the supernatant fluid, were fixed as described above.

Samples for preparation of thin sections were postfixed for 2 h in a 1% solution of OsO_4 in 0.2 M s-collidine buffer (pH 7.4), dehydrated with ethanol, cleared with propylene oxide, and embedded in Epon (33). Thin sections were cut with a diamond knife and post-stained with 2% aqueous uranyl acetate for 30 min (50), followed by 0.5% lead citrate for 10 min (20). Both stains contained a trace of Triton X-100 (8). In some instances (noted in figure legends) samples were prepared in the presence of Luft ruthenium red stain (38) or in the presence of Alcian blue and lanthanum nitrate (42). Thin sections were examined with a Philips EM 300 electron microscope. Thick (3 μm) sections were viewed with a Zeiss photomicroscope equipped with phase-contrast optics.

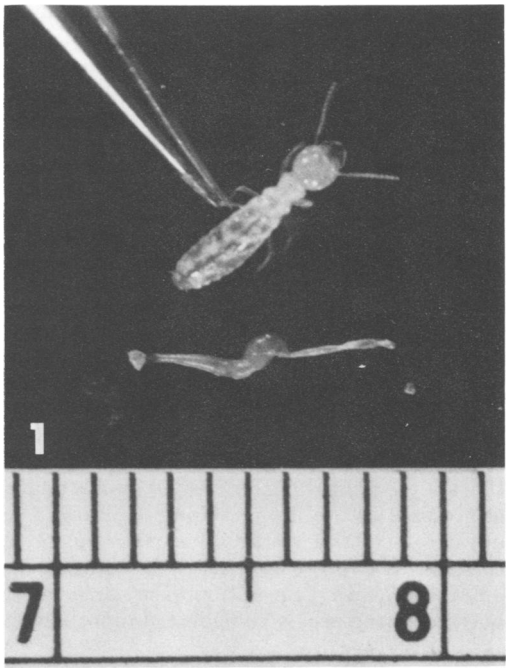

FIG. 1. *A live worker of R. flavipes is held next to an extracted gut from a separate worker. Anatomical regions of the extracted gut and ruler segments to which they correspond are: hindgut, 7.2 to 7.6 cm; midgut, 7.6 to 7.9 cm; paunch, 7.5 to 7.6 cm.*

Samples for SEM were dehydrated in graded concentrations of ethanol (70 to 100% in 10% increments) and then subjected to critical-point drying with CO_2 (3). Dried specimens were mounted on stubs and coated with gold before viewing with an AMR 900 scanning electron microscope.

Protozoa present in hindguts were identified by their morphology (29, 32) in wet mount (phosphate-buffered saline; see above) preparations, when viewed by phase-contrast microscopy.

Designation of bacterial morphotypes. Bacterial morphotypes observed only in *R. flavipes* or only in *C. formosanus* were assigned the prefix "R" or "C," respectively, followed by a number. Bacterial morphotypes observed in both termite species were assigned a number, without a letter prefix.

RESULTS

General morphology of the paunch of laboratory-maintained (LM) worker termites and its microbiota. Hindguts of *R. flavipes* and *C. formosanus* workers were approximately 4 mm long and 0.5 to 1 mm in diameter at their widest point, which was the paunch region (Fig. 1). Phase-contrast microscopy of wet mount preparations of paunch contents revealed an abun-

dance of motile and nonmotile bacteria, along with major species of protozoa typically associated with these termites (i.e., *Pyrsonympha vertens*, *Dinenympha gracilis*, and *Trichonympha agilis* in *R. flavipes*, and *Pseudotrichonympha grassii*, *Holomastigotoides hartmanni*, and *Spirotrichonympha leidyi* in *C. formosanus*). An indication of the abundance of protozoa in the termite paunch was obtained by SEM (Fig. 2). In the paunch of *R. flavipes*, *P. vertens* was usually situated at the periphery of the lumen contents, with its anterior end oriented toward the epithelial surface (Fig. 2), suggesting that some cells might be attached to this tissue. Filaments, present among the protozoa of *R. flavipes* (Fig. 2), proved to be bacterial trichomes (see below).

Phase-contrast microscopy of transverse sections of the paunch also revealed an abundance of protozoa in the lumen. However, careful examination of the epithelial surface suggested that it was densely covered with bacteria, and TEM confirmed this notion (Fig. 3, 5, 6). In both termite species considerable morphological heterogeneity was apparent for the bacteria that consisted of straight and slightly curved rods, undulate and endospore-forming cells, pleomorphic coccoid bacteria, and spirochetes. A number of bacteria appeared to be undergoing fission. Some bacterial aggregates in *C. formosanus* were clearly entrapped within a fibrous matrix of moderate electron density (Fig. 5). TEM also revealed the thinness of the paunch epithelium as in Fig. 3, which showed it to be a single layer of cells about 4 μm thick.

Cup-shaped depressions, measuring 2 to 4 μm in diameter and 1 to 2 μm deep, were present in the epithelial surface (Fig. 3, 7 to 9). The cuticle of the epithelium was continuous with the concavity of cups. In addition, the epithelial cell membrane adjacent to cups displayed numerous invaginations which, in turn, were interposed with elongate mitochondria approximately 0.1 μm in diameter (Fig. 3, 4, 7). Hemispherical aggregates of bacteria were frequently centered at the cups: a portion of one is shown in Fig. 3 to extend radially about 17 μm from the center of the cup. In both *R. flavipes*

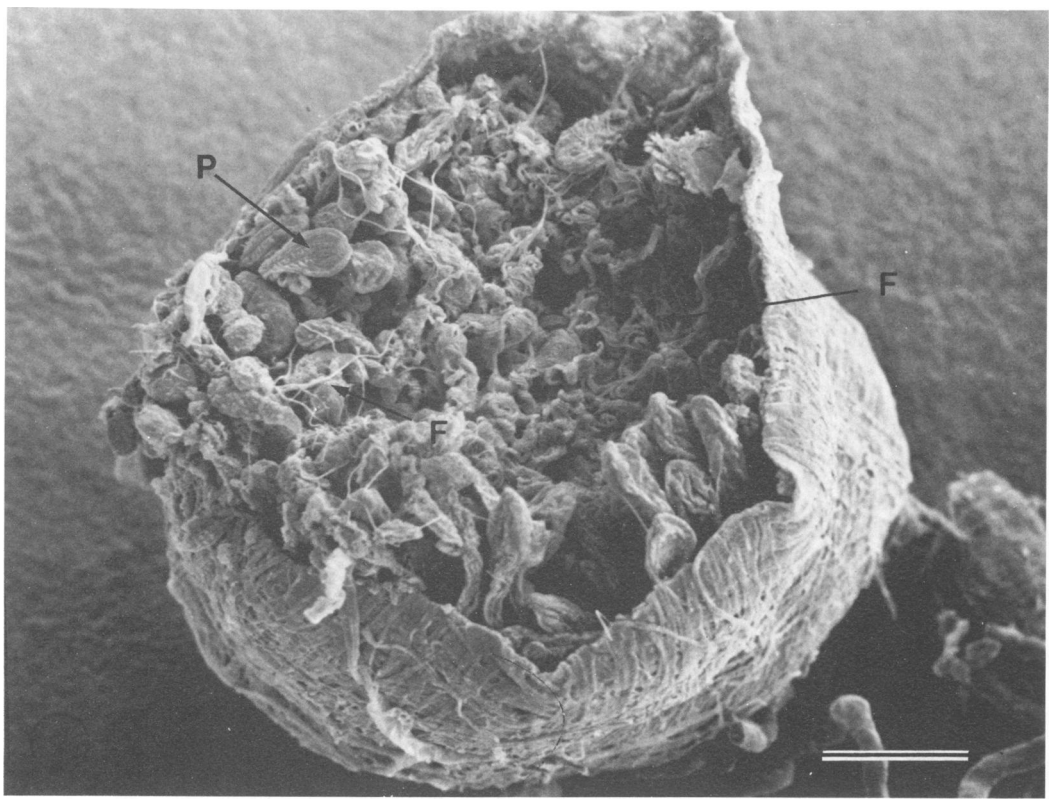

FIG. 2. *Scanning electron micrograph of a cross section through the paunch of an R. flavipes worker. Note the abundance of protozoa, with P. vertens (P) oriented with its anterior (tapered) end toward the epithelium. Bacterial filaments (F) are present among the protozoa. Bar = 100 μm.*

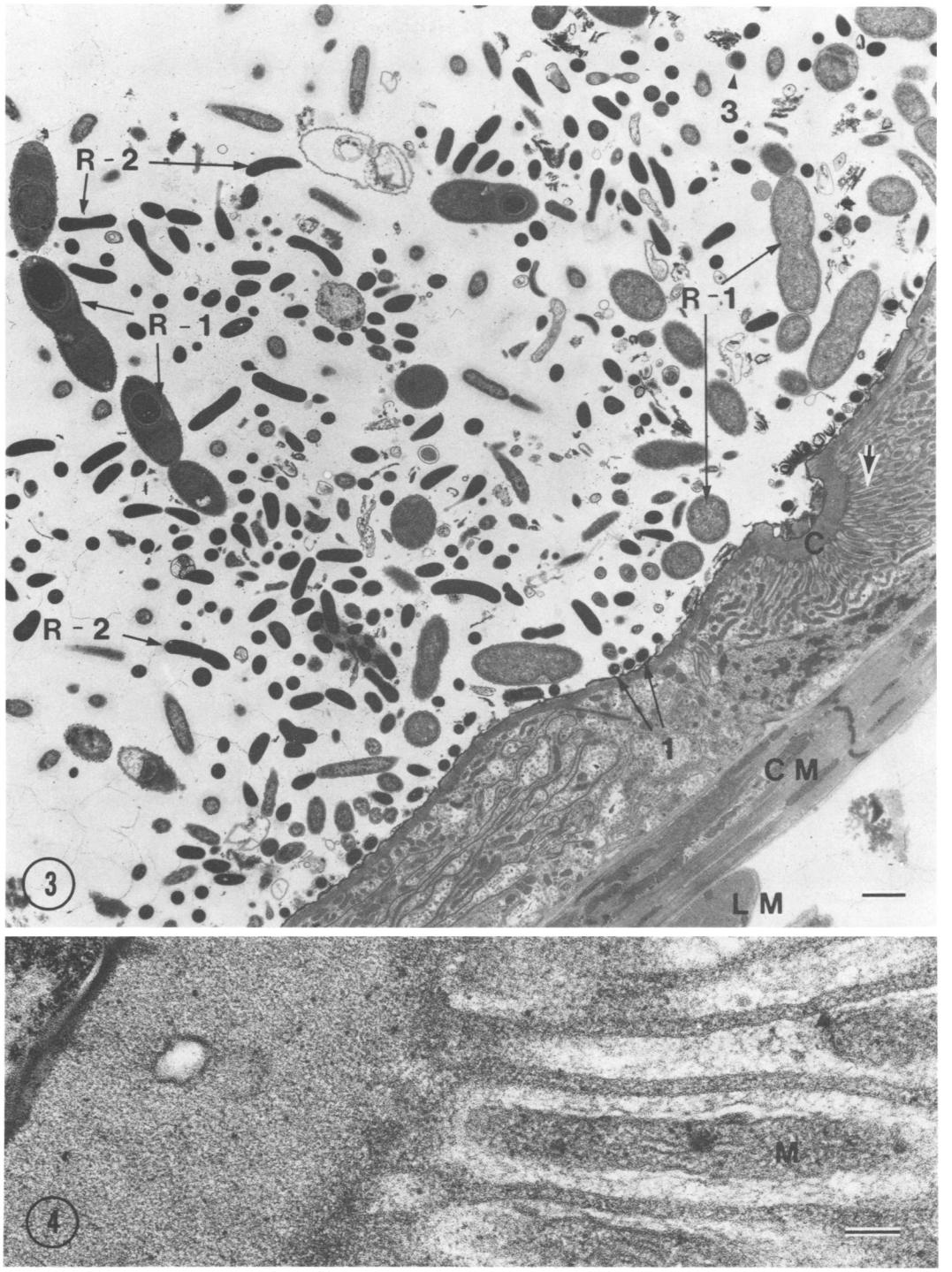

FIG. 3. *Transmission electron micrograph of the paunch epithelium of R. flavipes and its associated microbiota. A portion of a hemispherical aggregate of bacteria is centered at a cuplike depression (C) in the epithelium. Mitochondria are concentrated near the cup amid invaginations of the cytoplasmic membrane (arrowhead). Bacterial morphotypes 1, 3, R-1, and R-2 are labeled. CM, Circular muscle fibers; LM, longitudinal muscle fibers. Bar = 1 μm.*

FIG. 4. *Detail of region shown at arrowhead in Fig. 3. M, Mitochondrion. Bar = 0.1 μm.*

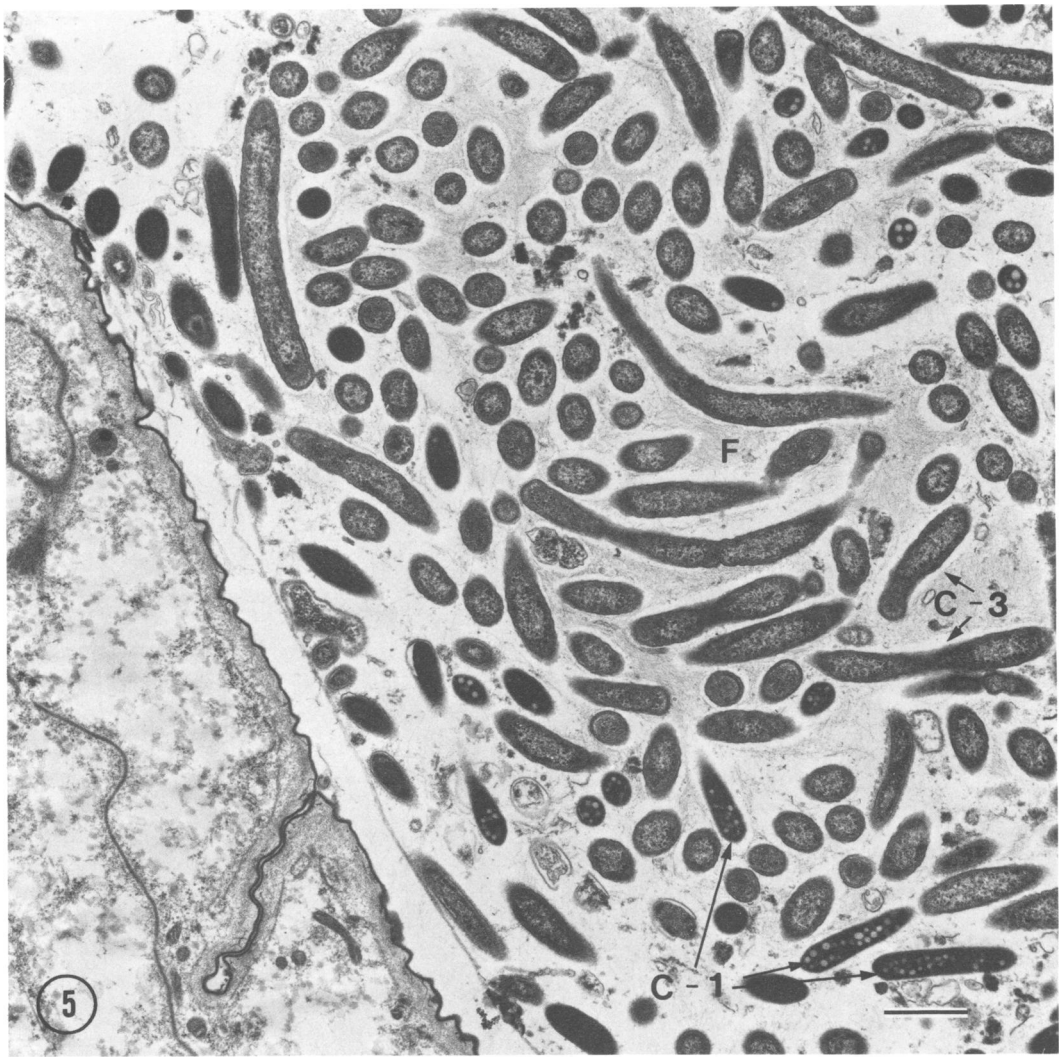

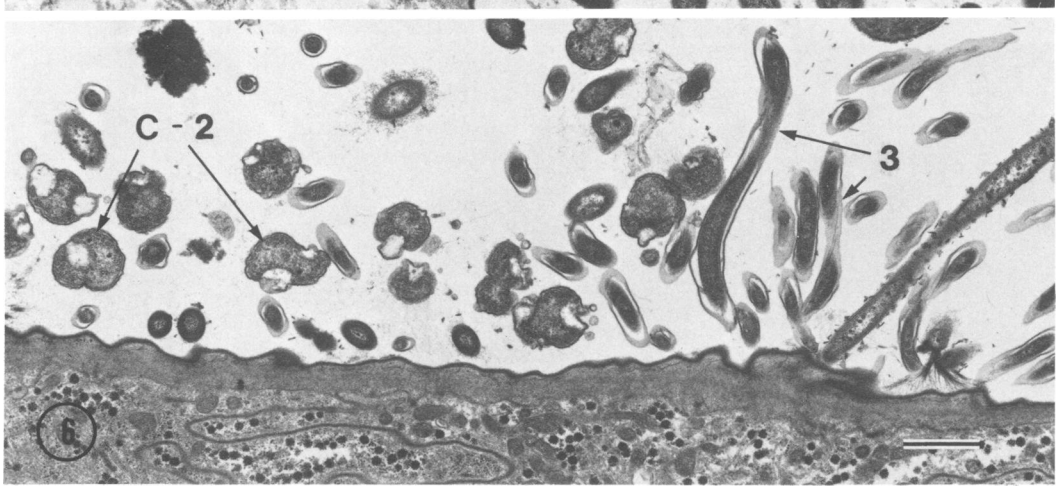

FIG. 5. *Transmission electron micrograph of a portion of a bacterial aggregate associated with the paunch epithelium of C. formosanus. Fibrous material (F) is prominent around cells of morphotype C-3. Morphotype C-1 cells are also present. Bar = 1 μm.*

FIG. 6. *Transmission electron micrograph of bacterial morphotypes 3 and C-2 situated near the paunch epithelium of C. formosanus. Ruthenium red. Bar = 1 μm.*

and *C. formosanus*, cups contained varying amounts of electron-dense, granular material (Fig. 7 to 9; see Fig. 26). When cups were filled with such material, rods and undulate bacteria were often positioned at cups such that one pole of the cells was closely associated with the granular substance (Fig. 7 and 9).

The chemical nature of the granular material in cups is not known. Although first thought to be mucopolysaccharide, attempts to stain the material with ruthenium red or a combination of Alcian blue and lanthanum nitrate yielded inconclusive results. Ruthenium red treatment did, however, enhance the overall contrast of transmission electron micrographs when combined with the usual post-staining of grids and was therefore used in the preparation of many of the micrographs.

Noteworthy was the presence of bulbous protuberances on the concave surface of cups seen by both TEM (Fig. 7 to 9, 26) and SEM (see Fig. 13). It appeared that the granular material present in cups was extruded from the protuberances (Fig. 8, 9, 26).

SEM of the paunch epithelium of LM worker termites. Because cups were a prominent feature of the paunch epithelium and sites for aggregation of bacteria, it was of interest to determine their number and arrangement. This quest, which utilized SEM, also revealed the strong adherence of bacteria to the epithelium. When sliced gut segments were gently agitated in phosphate-buffered saline, many bacteria remained attached to the paunch epithelium (Fig. 10). Microcolonies of bacteria were clearly discernible (Fig. 10 and 11). Some microcolonies consisted of morphotype 1 (see Table 3) cells which were thin rods (Fig. 10). Others consisted of rods (undesignated) thicker than morphotype 1, which possessed thread- or knoblike appendages (Fig. 11). Although a suggestion of epithelial cups was obtained in such preparations (Fig. 10), the dense coating of bacteria precluded accurate estimates of intercup distance. Agitation of gut segments with a Vortex mixer removed many bacteria and exposed some cups; however, numerous clumps of bacteria still remained on the epithelium. Best results were obtained when guts were prepared from termites fed antibiotics for 10 days. Such preparations were almost entirely bacteria-free and showed cups to have a fairly regular arrangement on the epithelium (Fig. 12). The average linear distance between adjacent cups was 12.0 ± 0.8 μm (*R. flavipes*) and 11.9 ± 2.4 μm (*C. formosanus*). Approximating the paunch to a cylinder 0.5 mm in diameter by 1 mm in length and taking the average distance between adjacent cups to be 12 μm, it was calculated that about 11,000 cups were present on the paunch epithelium. The diameter of cups measured by SEM averaged 1.5 μm, which agreed well with measurements made by TEM. Protuberances, presumably identical to those seen by TEM (Fig. 7 to 9, 26), were visible on the concave surface of cups. About 40 such protuberances were present in the cup shown in Fig. 13.

Epibiontic relationships among paunch bacteria of *R. flavipes*. SEM and TEM of the paunch microbiota of *R. flavipes* revealed an intimate physical association between thin (0.36 by 2.2 μm) rod-shaped bacteria with tapered ends and thicker trichomes consisting of chains of rods (1.4 by 2.1 μm) (Fig. 14 to 17). The thin rods (termed epibionts and designated as morphotype R-5 [Table 1]) were aligned with their long axis essentially parallel with the long axis of trichomes (designated as morphotype R-4 [Table 1]) (Fig. 14). At times, epibionts covered almost the entire surface of trichomes (Fig. 14). TEM of thin sections of the paunch revealed that clusters of trichomes, with adherent epibionts, were usually positioned 16 to 20 μm from the epithelial surface. TEM also revealed the presence, in trichomes, of structures similar in appearance to bacterial endospores (Fig. 16).

Attachment of epibionts to trichomes appeared to be mediated by fibrous, holdfast material that emanated from the former (Fig. 15 to 17). Holdfast material was present around the entire surface of epibionts, but was most pronounced in regions where the surface of epibionts was in close proximity to that of the trichome (Fig. 15 to 17).

The cell envelope of epibionts was complex and typical of that of gram-negative bacteria (18). The envelopes consisted of an inner (cytoplasmic) and outer (wall) membrane (Fig. 15 and 17). The two membranes were separated by a space of about 20 nm, in which was observed a faint layer of moderate electron density. The cell wall of individual rods which made up trichomes, however, was more like a gram-positive type (Fig. 15 to 17). In addition, cells of the trichome were contained within a continuous wall layer (Fig. 16 and 17).

Bacterial morphotypes commonly observed in the paunch of LM worker termites. During these studies it became obvious that certain morphological types of bacteria were routinely observed in the paunch of one or both worker termite species. It was therefore of interest to investigate their in situ morphology in greater detail. Attention was directed to those bacteria

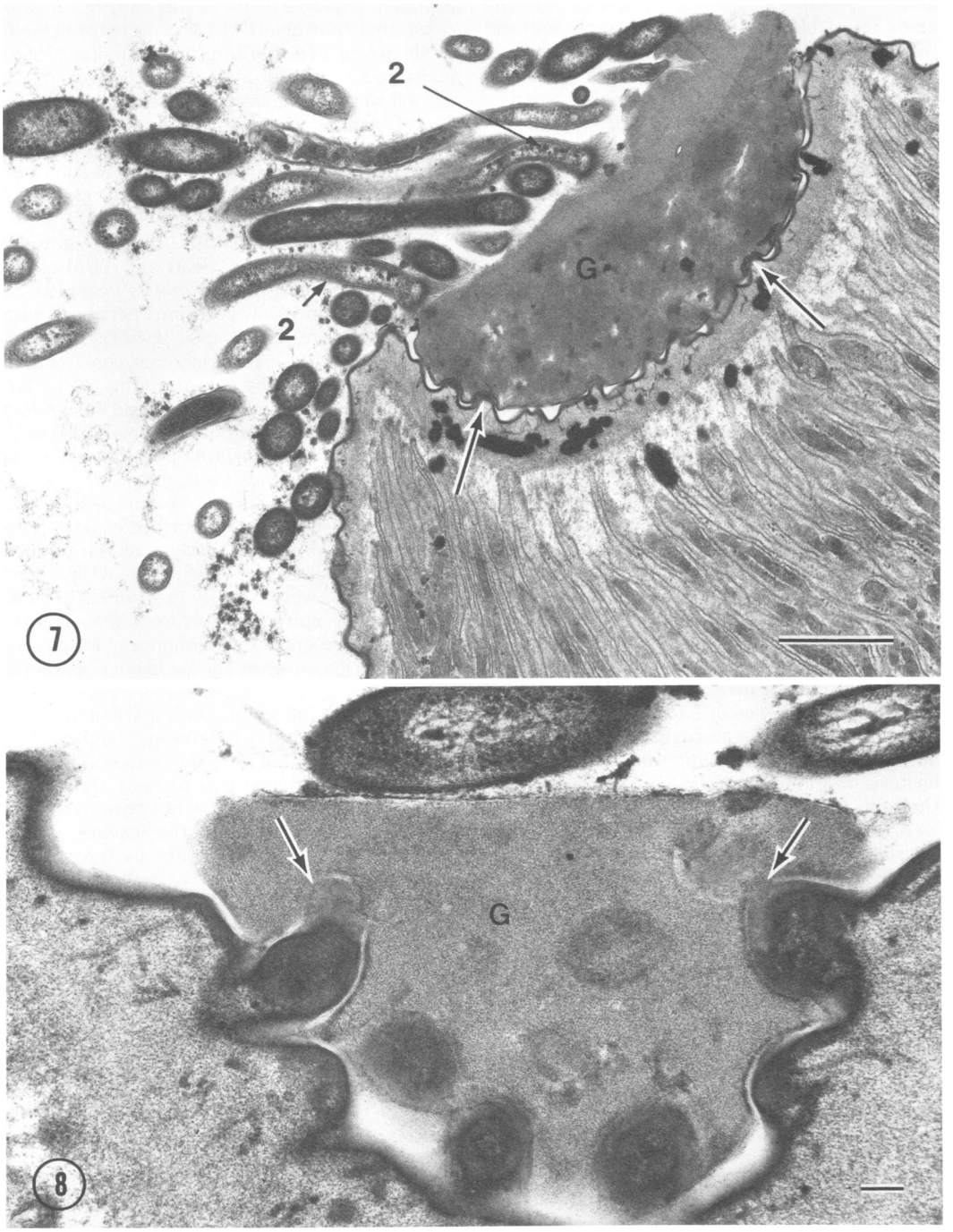

FIG. 7. *Transmission electron micrograph of an epithelial cup of C. formosanus. Morphotype 2 cells are intimately associated with the granular material (G) within cups by means of polar fibrils. Note the bulbous protrusions (unlabeled arrows) on the concave cup surface. Ruthenium red. Bar = 1 μm.*

FIG. 8. *Transmission electron micrograph of granular material (G) within an epithelial cup of C. formosanus. Bulbous protrusions on the concave surface of the cup may exude the granular material (arrows). Ruthenium red. Bar = 0.1 μm.*

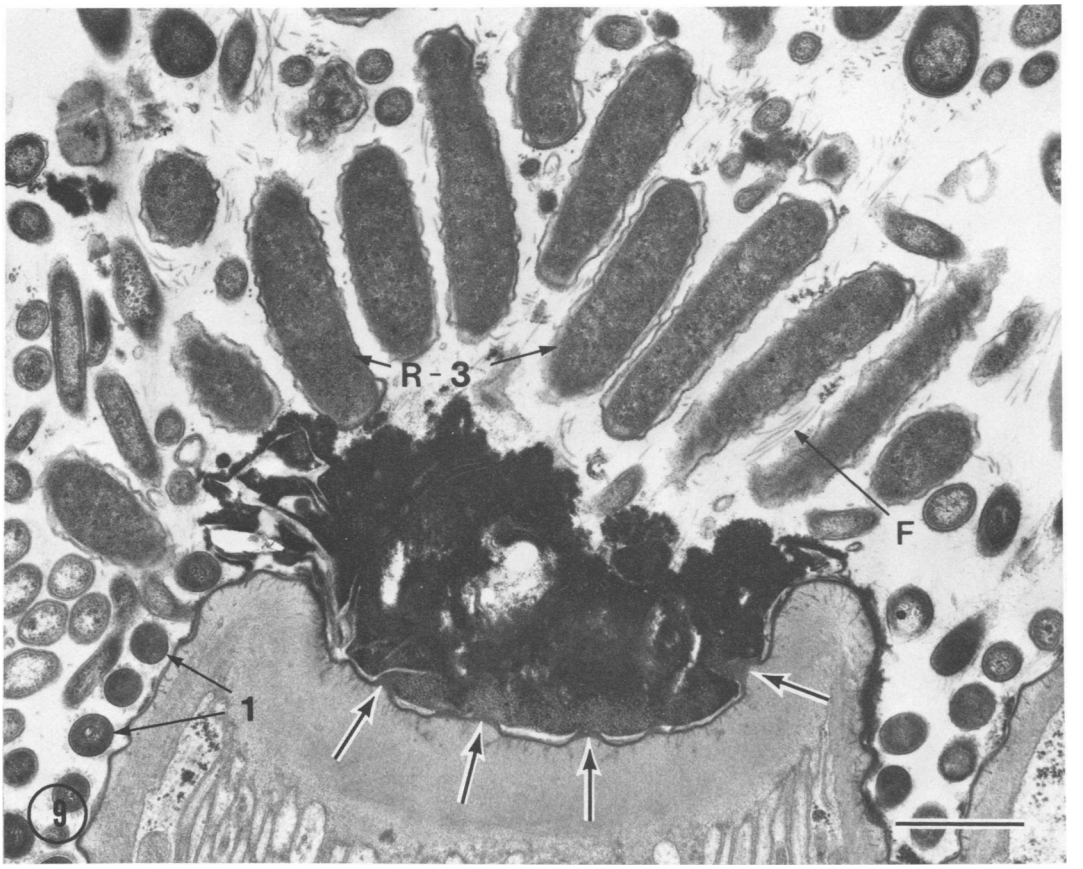

FIG. 9. *Transmission electron micrograph of an epithelial cup of R. flavipes with an associated cluster of R-3 cells. Note the granular material adjacent to protuberances (unlabeled arrows) similar to that shown in Fig. 8. Morphotype 1 cells are also evident. F, Flagella-like filaments. Ruthenium red. Bar = 1 μm.*

that were intimately associated with the paunch epithelium or with each other and/or possessed distinctive ultrastructural features that facilitated their recognition.

(i) ***R. flavipes* workers.** Bacterial morphotypes commonly observed in LM *R. flavipes* workers and not in *C. formosanus* were R-1 through R-5 (Table 1).

R-1 cells were elliptic, endospore-forming rods (1.2 by 2.3 μm) frequently observed in bacterial aggregates near the paunch epithelium (Fig. 3 and 19). Besides their overall shape, size, and frequent presence of endospores, they also exhibited a wavy outer cell wall layer (Fig. 19).

R-2 cells, usually present in bacterial aggregates (Fig. 3 and 19), were densely staining, slightly curved rods (0.35 by 1.1 to 1.5 μm) that possessed fibrous appendages at their poles. Appendages were often in contact with other bacteria (Fig. 19) and may function in attachment.

R-3 cells were rods (0.6 by 1.7 to 2.5 μm) associated with the paunch epithelium and often aggregated near granular material present in epithelial cups (Fig. 9). R-3 was distinguished by its overall shape and dimensions, as well as by the wavy contour of its outer cell wall layer. Endospores were never observed in R-3, although filaments measuring about 10 nm and which may be flagella were always numerous in the vicinity of R-3 cells (Fig. 9).

Morphotypes R-4 and R-5 refer to the endospore-forming trichomes and their epibionts, respectively, described in the section on epibiontic relationships (above).

(ii) ***C. formosanus* workers.** Bacterial morphotypes commonly observed in LM *C. formosanus* workers, but not in *R. flavipes*, were C-1 through C-3 (Table 2).

Morphotype C-1 cells were densely staining rods (0.32 by 1.4 μm) routinely present among bacterial aggregates on the paunch epithelium (Fig. 5 and 21). C-1 possessed no apparent fla-

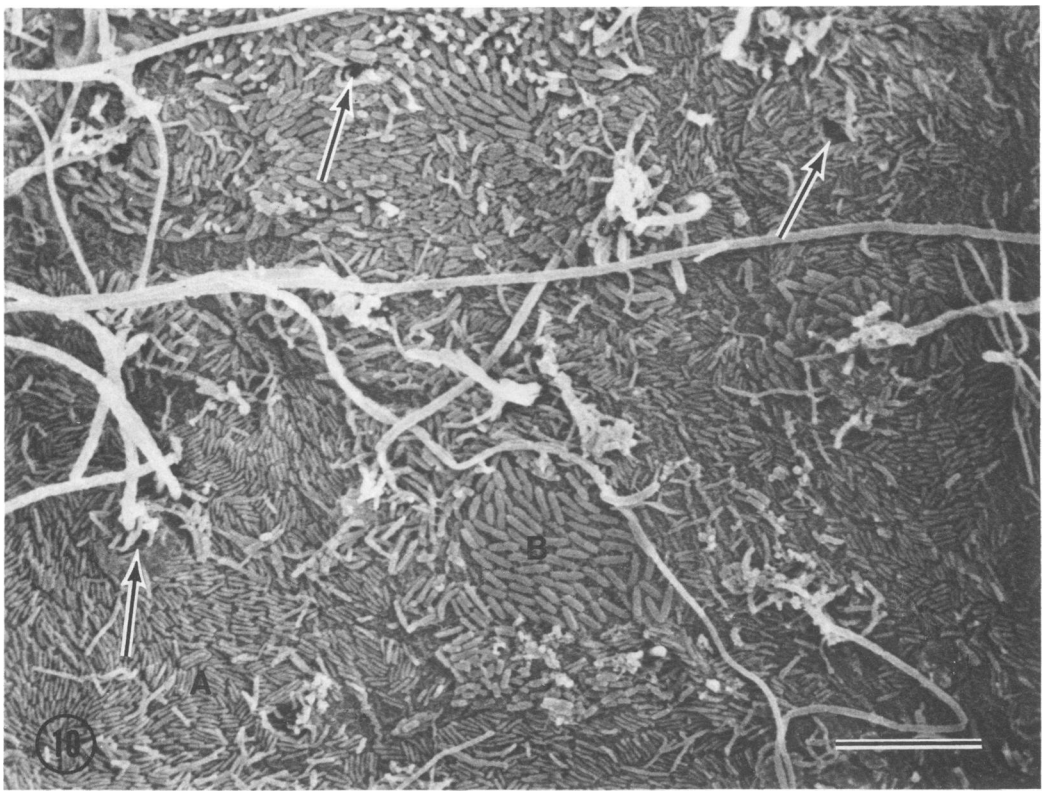

FIG. 10. *Scanning electron micrograph of the paunch surface of R. flavipes after gentle agitation in phosphate-buffered saline. A suggestion of epithelial cups may be seen (arrows). A microcolony of morphotype 1 cells (A) and that of an undesignated morphotype (B) are evident. Bar = 10 μm.*

gella or fibrous extensions of the cells, but contained numerous intracellular granules similar in appearance to those of poly-β-hydroxybutyrate (49). An indication of a limiting membrane around granules was observed (Fig. 21).

Morphotype C-2 cells were pleomorphic, coccoid organisms measuring 0.6 to 0.8 μm in diameter (Fig. 6 and 22). The cytoplasmic membrane of C-2 was closely apposed to the cell wall at most regions. However, at one or more sites the cytoplasmic membrane was markedly pulled in from the wall by about 0.3 μm (Fig. 22). The resulting region was relatively electron translucent. Whether the vacuolated appearance of C-2 reflected a fundamental attribute of cells or was merely the result of plasmolysis during specimen preparation is not known. However, the vacuolation served as a useful feature for readily recognizing cells of this morphotype.

Morphotype C-3 cells were curved rods (0.45 by about 3.5 μm) usually present as aggregates on the epithelium (Fig. 5). C-3 cells were embedded in fibrous material which they appeared to produce. Consistent with this interpretation was the greater relative abundance of fibers around cells of C-3 as opposed to cells of other morphologies shown in the lower right and upper left corners of Fig. 5.

(iii) Bacterial morphotypes common to both *R. flavipes* and *C. formosanus*. Bacterial morphotypes 1 through 3 were observed in the paunch of both termite species (Table 3).

Morphotype 1 cells were thin, densely staining rods (0.34 by 0.9 to 2.0 μm) usually closely apposed to the paunch epithelium (Fig. 3, 9, 10, 18, 22). Cells possessed a fuzzy, electron-dense coating over their entire surface, which appeared to mediate their attachment to the epithelium and to each other (Fig. 18).

Morphotype 2 cells were curved to undulate rods 0.32 μm in diameter, which had an array of fibers associated with at least one pole of the cell (Fig. 7, 20, 22). The length of the organisms (>4 μm) plus their undulate shape made it impossible for us to obtain longitudinal sections through an entire cell. Consequently, we are uncertain as to whether fibers emanate from

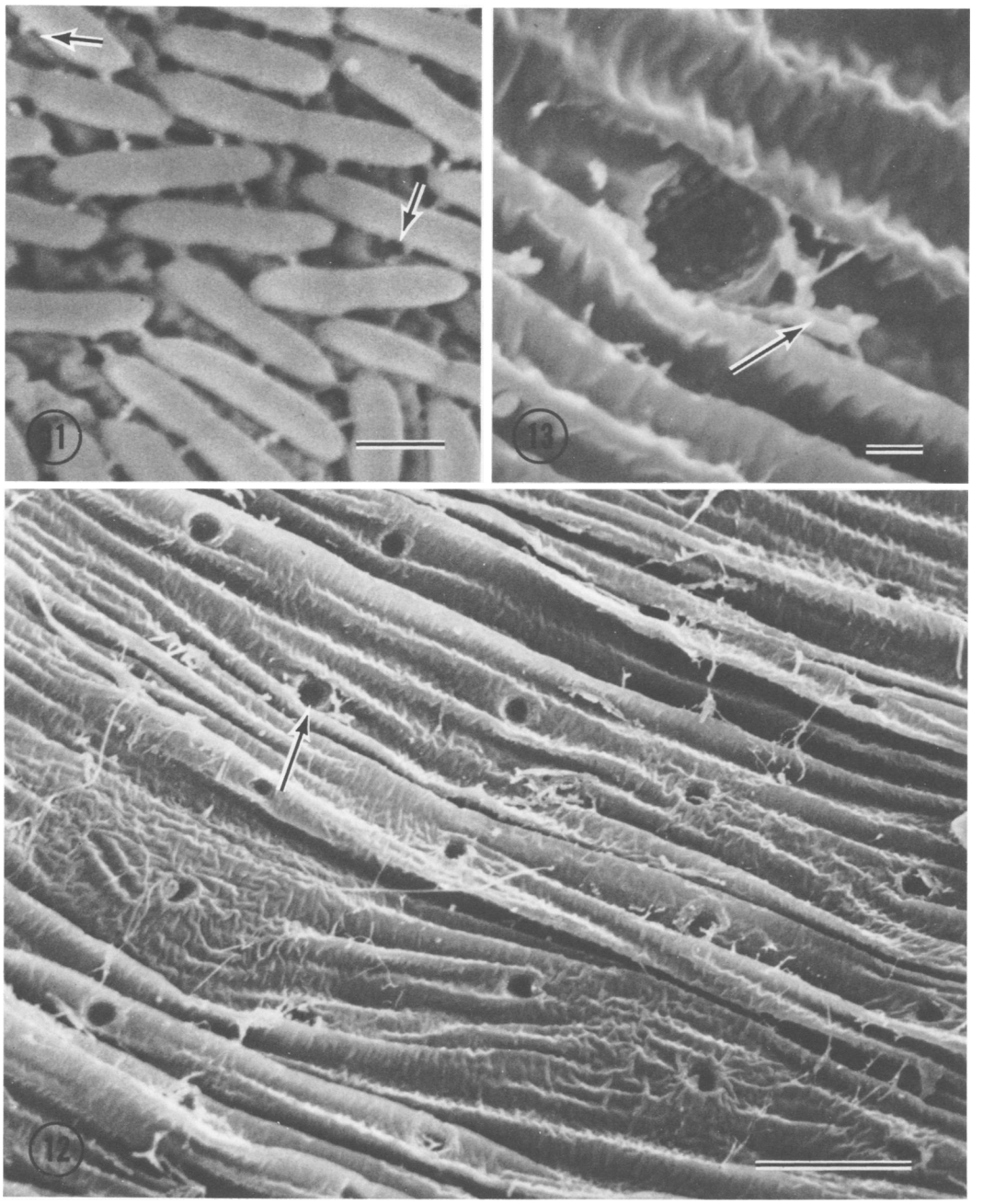

FIG. 11. *Higher-magnification micrograph of microcolony B shown in Fig. 10. Note the thread- or knoblike appendages making contact with neighboring cells and also with the epithelium (arrows). Bar = 1 μm.*

FIG. 12. *Scanning electron micrograph of the paunch epithelium of antibiotic-fed C. formosanus. Cups are clearly visible in the epithelial surface. Cup at arrow is shown at higher magnification in Fig. 13. Bar = 10 μm.*

FIG. 13. *Detail of indicated cup in Fig. 12. Bulbous protuberances are clearly seen on the concave cup surface. A few bacteria (arrow) remain near the cup. Bar = 1 μm.*

TABLE 1. *Bacterial morphotypes observed only in the paunch of R. flavipes*

Morphotype	Major characteristics	Termite specimens[a]	Relevant figures
R-1	Elliptic rod (1.2 by 2.3 μm), endospores formed, wavy outer cell wall layer	LM: W; FS: W, S	3, 19
R-2	Slightly curved rod (0.35 by 1.1 to 1.5 μm), possess polar fibrils	LM: W; FS: W, S	3, 19
R-3	Rod (0.6 by 1.7 to 2.5 μm), wavy outer wall layer, may possess flagella	LM: W; FS: W, S	9
R-4	Trichome-forming rod (1.4 by 2.1 μm), endospores formed	LM: W; FS: W	14, 15, 16, 17
R-5	Rod (0.36 by 2.2 μm), tapered ends, epibiontic on morphotype R-4	LM: W; FS: W	14, 15, 16, 17
R-6	Oval to rodlike (0.5 by 1.0 μm), wavy cell surface layer, cytoplasmic inclusions	LM: W; FS: W, S	23
R-7	Curved rod (0.42 by 2.1 to 3.8 μm), loose-fitting outer membrane, single polar flagellum, cytoplasmic inclusions	LM: W; FS: W, S	24, 25, 26

[a] LM, Laboratory maintained; FS, field specimens; W, worker; S, soldier.

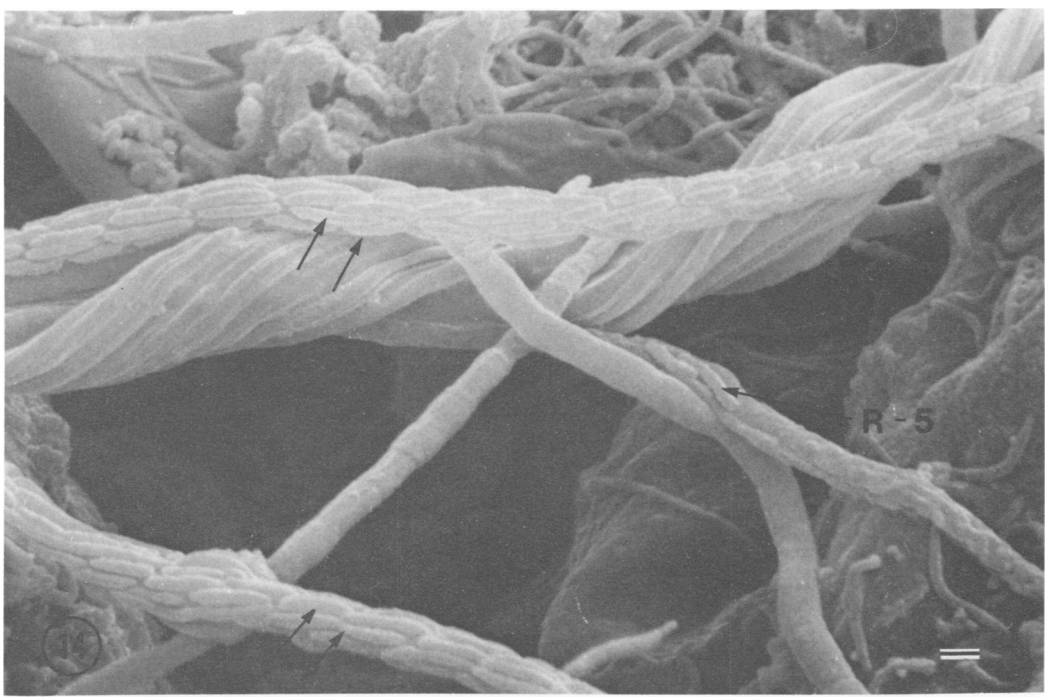

FIG. 14. *Scanning electron micrograph of bacterial trichomes with adherent epibionts (morphotype R-5) present in the paunch lumen of R. flavipes. Trichomes were often almost completely covered with epibionts (double arrows). Bar = 1 μm.*

both poles. Morphotype 2 adhered to the paunch epithelium and to granular material within epithelial cups with the aid of their fibrous appendages (Fig. 7, 20, 22). The cell envelope of morphotype 2 was complex and of the gram-negative type (18). The cytoplasmic membrane was separated from an outer (wall) membrane by a space of about 20 nm which in turn contained a poorly defined layer of moderate electron density (Fig. 20 and 22). In addition, a ribbed surface layer or sheath was separated from the outer wall membrane by about 16 nm (Fig. 20 and 22). The ribbed appearance of the sheath was best seen in oblique-sectioned cells (Fig. 22), whereas the sheath exhibited a "sawtooth" appearance in cells sectioned longitudinally (Fig. 20). The sheath was poorly defined at the fibril-containing pole of cells (Fig. 20 and 22).

An abundance of spirochetes was always present in the paunch of both termite species. Their size varied (0.2 by 3 μm to 0.5 by 10 to 20

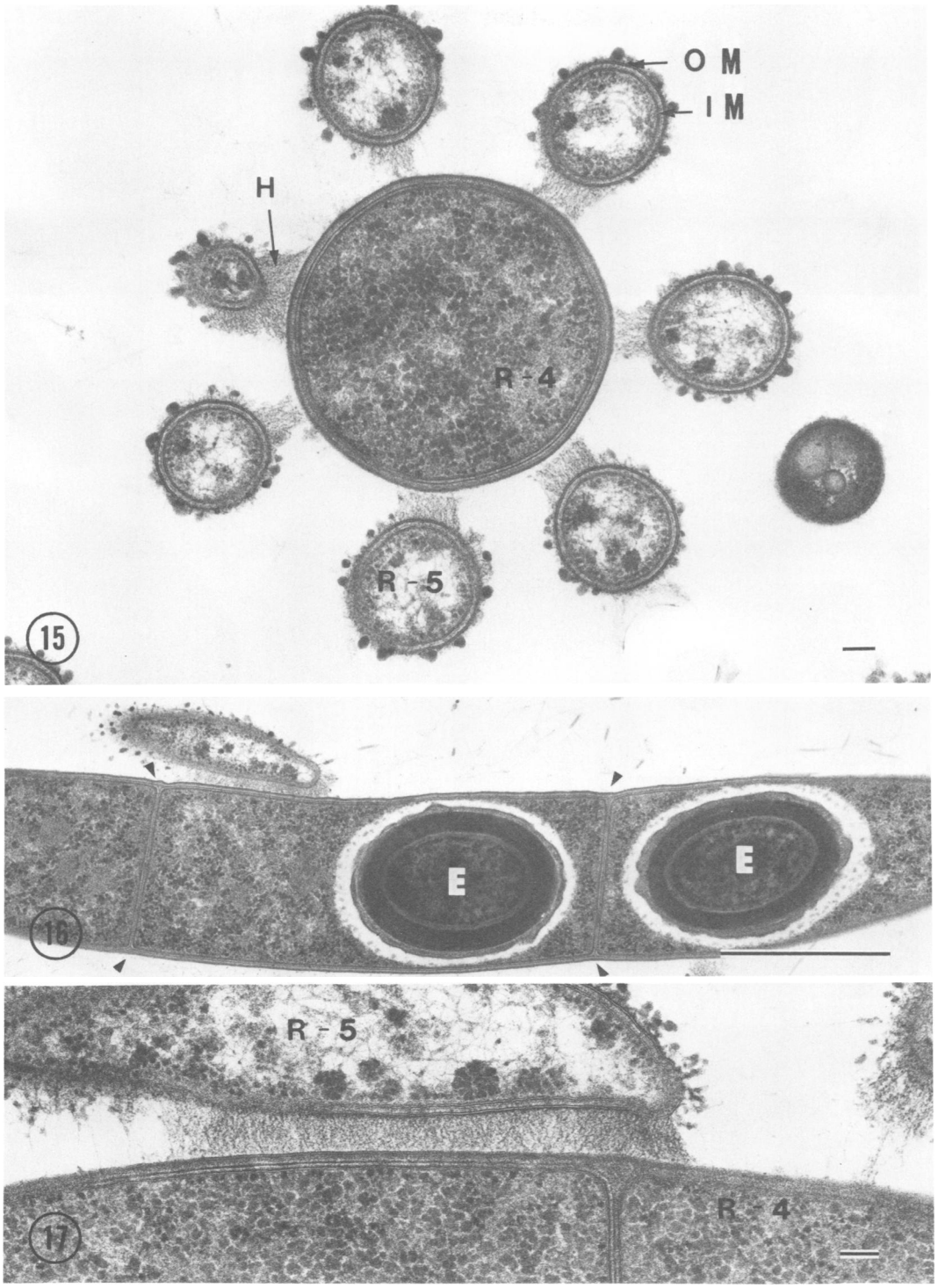

FIG. 15, 16, AND 17. *Thin sections through trichomes (R-4) showing adherence of epibionts (R-5) by means of fibrous holdfast material (H) that emanates from the latter. Note the tapered ends of epibiont cells. Arrowheads (Fig. 16) indicate the continuity of the outer layer of trichomes. IM, Inner (cytoplasmic) membrane; OM, outer (wall) membrane; E, endospore. Ruthenium red. Bars = 0.1 μm (Fig. 15 and 17) and 1 μm (Fig. 16).*

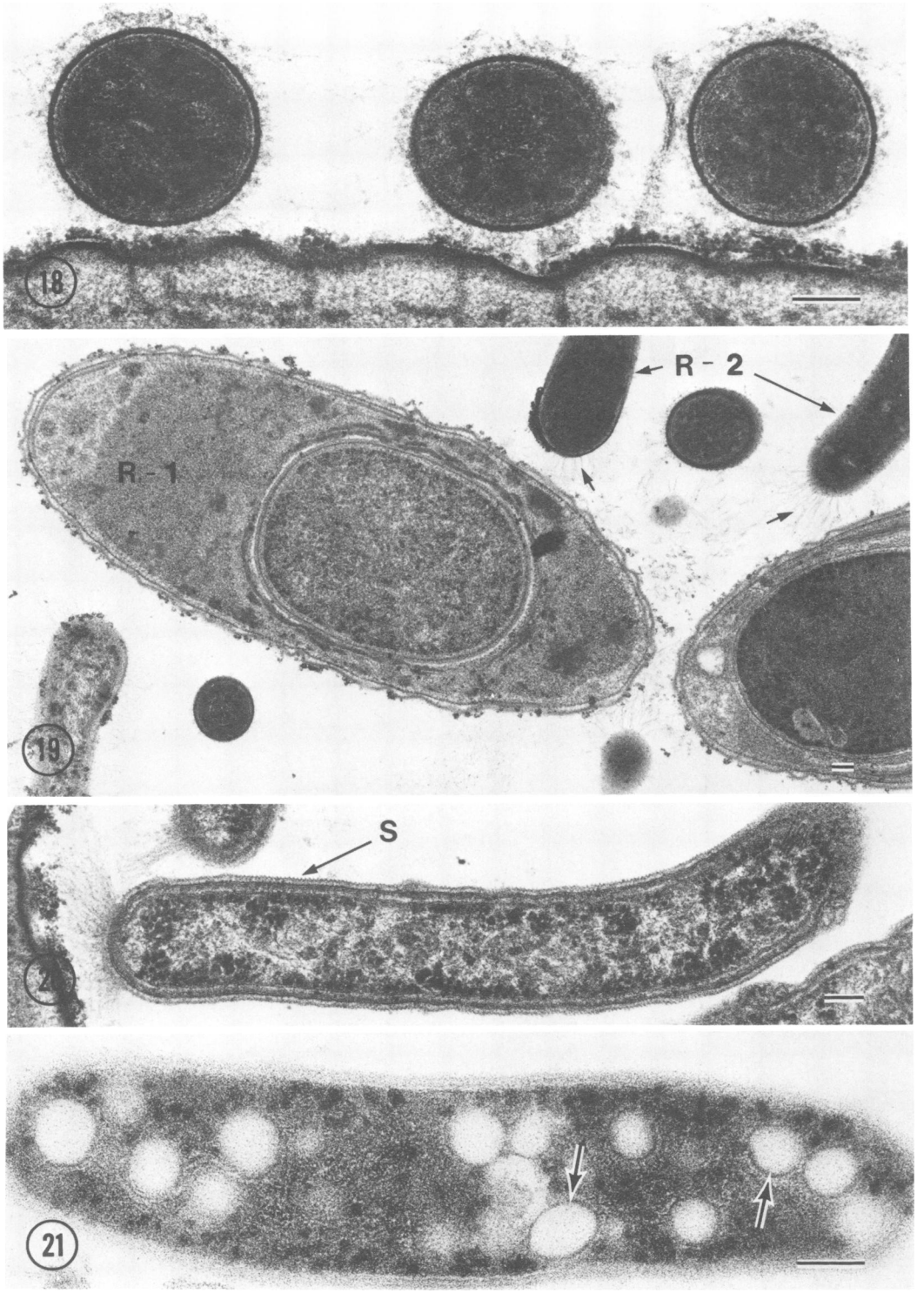

FIG. 18. *Transverse section of morphotype 1 cells in R. flavipes. A fuzzy, electron-dense coat around cells appears to mediate adherence to the paunch epithelium. Bar = 0.1 μm.*

FIG. 19. *Transmission electron micrograph of morphotype R-1 and R-2 cells from R. flavipes. Endospores are frequently present in R-1 cells. Fibrous, polar appendages (unlabeled arrows) of R-2 cells appear to mediate adherence to other cells. Bar = 0.1 μm.*

FIG. 20. *Transmission electron micrograph of a morphotype 2 cell with polar fibers contacting the epithelium at left. Note the "sawtooth" appearance of the outer sheath (S). Bar = 0.1 μm.*

FIG. 21. *Longitudinal section of a morphotype C-1 cell. Electron-translucent granules are abundant in the cell. An indication of a limiting membrane (arrows) around granules may be seen. Bar = 0.1 μm.*

μm), as did the degree of coiling or waviness of the cells. Spirochetes were rarely in close contact with the epithelium and were only rarely observed among bacterial aggregates on the epithelium (Fig. 3, 6, 22). However, because they possessed distinctive morphological features common to all known spirochetes (i.e., protoplasmic cylinder, axial fibrils, and outer sheath [12]), we refer to them collectively as morphotype 3, regardless of cell size or overall shape.

Paunch microbiota of *R. flavipes* samples from natural environments. It seemed possible that the overall morphology of the paunch microbiota might differ in termites sampled directly from nature. Our ready access to natural infestations of *R. flavipes* allowed us to test this possibility. This venture also afforded an ideal opportunity to examine the gut microbiota of colony members other than workers (e.g., larvae, soldiers, and alates).

(i) Workers and soldiers. The paunch microbiota of workers and soldiers was similar. However, TEM revealed significant differences in the biota from these specimens (Fig. 23 and 26) as compared with that from LM specimens (Fig. 3 and 9). Whereas cells of morphotypes 1, 2, 3, R-1, R-2, and R-3 were always present, as in LM workers, the epithelium was also colonized by oval to rod-shaped bacteria (0.5 by 1 μm) designated R-6 (Fig. 23; Table 1). R-6 cells contained numerous cytoplasmic inclusions, similar to poly-β-hydroxybutyrate (49), which occupied a major volume of the cytoplasm of most cells. Higher-magnification micrographs (not shown) revealed that R-6 cells had a wavy cell surface layer and amorphous, electron-dense material associated with the cell surface. It is important to note that R-6 cells were present in LM workers, but were not prevalent.

Another morphotype abundant in field specimens, but only infrequently observed in LM termites, was R-7 (Fig. 24, 25, 26; Table 1). R-7 cells were curved rods (0.42 by 2.1 to 3.8 μm) that had a single polar flagellum and a loose-fitting outer membrane or sheath (Fig. 24, 25, 26). Oblique sections revealed striations on the outer membrane that ran diagonally to the long axis of cells (Fig. 25). In addition, the outer membrane appeared connected to the main protoplasmic body by peglike elements seen only at the flagellum-free pole of cells (Fig. 25). R-7 cells always possessed an abundance of electron-translucent granules in the cytoplasm (Fig. 24 and 26).

(ii) Larvae. The morphological diversity of bacteria present in the paunch of larvae was not as great as that of workers and soldiers.

TABLE 2. *Bacterial morphotypes observed only in the paunch of C. formosanus*[a]

Morphotype	Major characteristics	Relevant figures
C-1	Rod (0.32 by 1.4 μm), densely staining, cytoplasmic inclusions	5, 21
C-2	Pleomorphic coccoid cells (0.6 to 0.8 μm in diam), vacuolated areas prominent in cell	6, 22
C-3	Curved rod (0.45 by 3.5 μm), usually embedded in fibrous material	5

[a] Only LM workers examined.

However, morphotype 1 and 3 cells were present in all specimens examined. The former were typically intimately associated with the paunch epithelium.

(iii) Alates. Hindguts of alates were thin and fairly uniform in diameter (0.2 to 0.3 mm). The paunch region was noticeably less robust than that of workers. Although the morphological diversity of bacteria was similar to that of workers, qualitative estimates indicated that the number of bacteria per gut was less. All specimens, however, possessed an abundance of R-6 and morphotype 3 cells. The former were closely associated with the epithelium.

A summary of bacterial morphotypes present in the paunch of field specimens is included as part of Tables 1 and 3.

Attachment of protozoa to the paunch epithelium of *R. flavipes*. Bloodgood (10) recently described in detail an "attachment organelle" of *Pyrsonympha* which secured these protozoa to the hindgut epithelium of *R. tibialis*. However, Bloodgood et al. (11) did not observe such an organelle on *Pyrsonympha* from *R. flavipes* and did not observe attachment of *Pyrsonympha* to the hindgut of the latter termite species. By contrast, SEM of paunch preparations from our specimens of *R. flavipes* suggested that some *Pyrsonympha* cells might be attached to the epithelium (Fig. 2), and TEM provided clear evidence that attachment occurs (Fig. 27). *Pyrsonympha* were attached, via their attachment organelle, to the paunch epithelium of workers and soldiers, whether LM or field specimens were examined. The morphology of the attachment organelle was similar to that described by Bloodgood (10). However, the frequency of attachment was not as great as reported for *R. tibialis*. Indeed, in preliminary studies (13) we did not observe the phenomenon.

Bacteria associated with the midgut epithe-

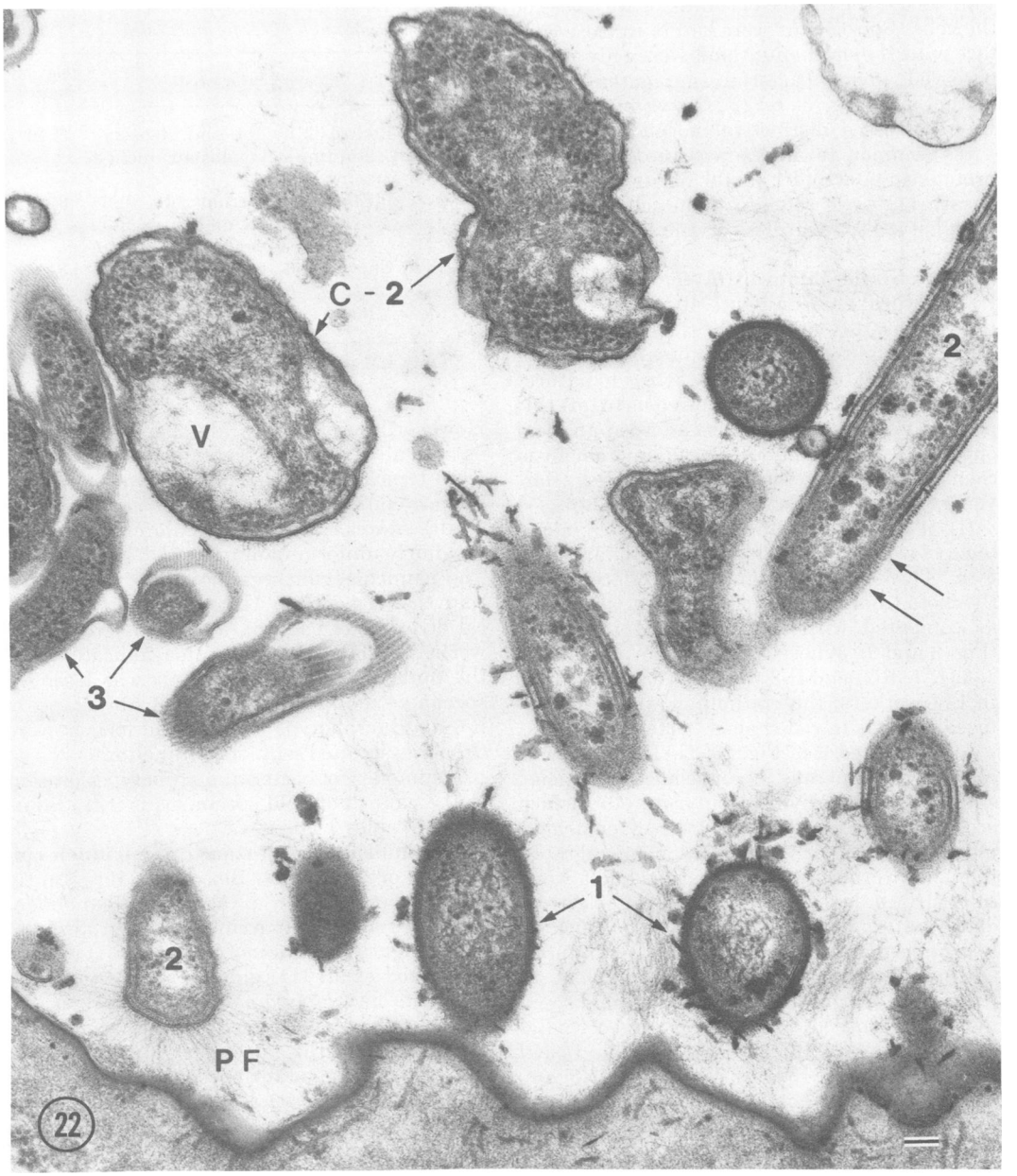

FIG. 22. *Transmission electron micrograph of a portion of the paunch epithelium of C. formosanus showing cells of morphotypes 1, 2, 3, and C-2. The ribbed nature of the sheath of morphotype 2 cells is seen in a partially oblique-sectioned cell (double arrows). Note the large vacuolated areas (V) in C-2 cells and the polar fibrils (PF) of morphotype 2 in contact with the epithelium. Ruthenium red. Bar = 0.1 μm.*

lium. Since a portion of the termite midgut was almost always attached to extracted hindguts (Fig. 1), thin sections were also made of this region and examined by TEM. Bacteria, consisting of a single morphotype (morphotype 4), were attached to the midgut epithelium of all termites examined (Table 3; Fig. 28 and 29). The organisms were rod-shaped or cuboidal, had a diameter of about 0.9 μm at their widest point, and were located between microvilli present on the epithelial surface. Occasional divided cells were seen (Fig. 28), and structures

TABLE 3. *Bacterial morphotypes common to both R. flavipes and C. formosanus*

Morphotype	Major characteristics	Location in gut[a]	Termites[b]		Relevant figures
			R. flavipes	*C. formosanus*	
1	Rod (0.34 by 0.9 to 2.0 μm), fuzzy surface coat seen by TEM	P	LM: W; FS: L, W, S, A	LM: W	3, 9, 10, 18, 22
2	Curved to undulate rod (0.32 by >4 μm), fibrous polar appendages, ribbed outer sheath	P	LM: W; FS: W, S	LM: W	7, 20, 22
3	Typical spirochete morphology (13), size range, 0.2 by 3 μm to 0.5 by 10 to 20 μm	P	LM: W; FS: L, W, S, A	LM: W	3, 6, 22
4	Rod-shaped to cuboidal (0.9 μm in diam), poorly defined cell wall layer, endospores present	M	LM: W; FS: L, W, S, A	LM: W	28, 29

[a] P, Paunch; M, midgut.
[b] LM, Laboratory maintained; FS, field specimens; L, larvae; W, workers; S, soldiers; A, alates.

similar to bacterial endospores were present in some cells (not shown). The cell wall of the bacteria, if present, was very poorly defined. The bacterial cell membrane was clearly separated from that of the epithelium by a space of 20 nm (Fig. 29). This space was occupied by amorphous, electron-dense material. The apical cytoplasm of epithelial cells near bacterial attachment usually lacked microvillar filaments which were present in adjacent areas (Fig. 28 and 29). No other organisms were observed to be associated with the midgut epithlium; likewise, few organisms were ever observed in the lumen of the midgut.

DISCUSSION

One aim of this study was to identify bacterial morphotypes that might constitute part of the autochthonous flora of the gut. Autochthonous microbes are those indigenous forms that colonize animals early in their lives, increase to relatively high populations, and remain at those populations throughout the lives of healthy animals (40). This was possible for *R. flavipes* since we had ready access to a variety of castes and developmental stages of this species. Pending enumeration by pure culture techniques, it was considered that morphotypes 1, 3, and 4 could be autochthonous in *R. flavipes*, because they were readily observed in all specimens from young larvae to sexually mature alates (Table 3). In addition, the ability of antibiotics to drastically decrease the bacterial population strongly suggested that bacteria were metabolizing and proliferating in the termite gut, a notion supported by the observation of dividing cells in guts and by the marked inhibitory effect of antibiotics on nitrogen fixation (14) and methanogenesis (13) by termites.

Phoresis, or the colonization by a microbe of the surface of another macro- or microorganism, is common in nature (2), and the attachment of organisms to gut epithelial tissues has been well documented for a variety of animal hosts (6, 15, 35, 39, 41, 46–48), including insects other than termites (21). The present findings extend the generality of this phenomenon since phoresis was apparent not only at the epithelial surface (Fig. 3, 5, 6, 9, 22, 23, 27, 28, 29), but also between different bacterial morphotypes (Fig. 14, 15, 16, 17, 19). Savage and Blumershine (41) suggested that phoresis of bacteria to intestinal epithelia affords a survival advantage to the adhering microbes, particularly in the "flowing stream" environment of the gut, where washout poses a threat to the structure and stability of the microbial community. Adherence would thus be a particular advantage to bacteria with low growth rates. However, in the termite paunch the ability of bacteria to adhere strongly to the epithelium would take on added importance, since not only must the colonizers resist washout due to food passage, but they must also contend with the disruptive, turbulent gyrations affected by the horde of protozoa (27) that is also present. It is noteworthy in this connection that phoresis between bacteria and termite gut protozoa is also common (5, 12). Although not investigated in this study, the interaction has been explored in detail by other workers (11, 17, 43–45).

Adherence of bacteria to the paunch or midgut epithelium or to other bacteria frequently appeared to be mediated by epicellular holdfast elements. Two general types of holdfast elements were observed. One type consisted of fuzzy, fibrous, or threadlike material which coated the entire surface of the cells and which was probably adhesive capsular or slime substance. Holdfast material of this nature has also been reported for other host-associated bacteria (1, 6, 15, 21, 34, 41). Another type of holdfast material consisted of a cluster of thin fibers that emanated from the poles of rod-

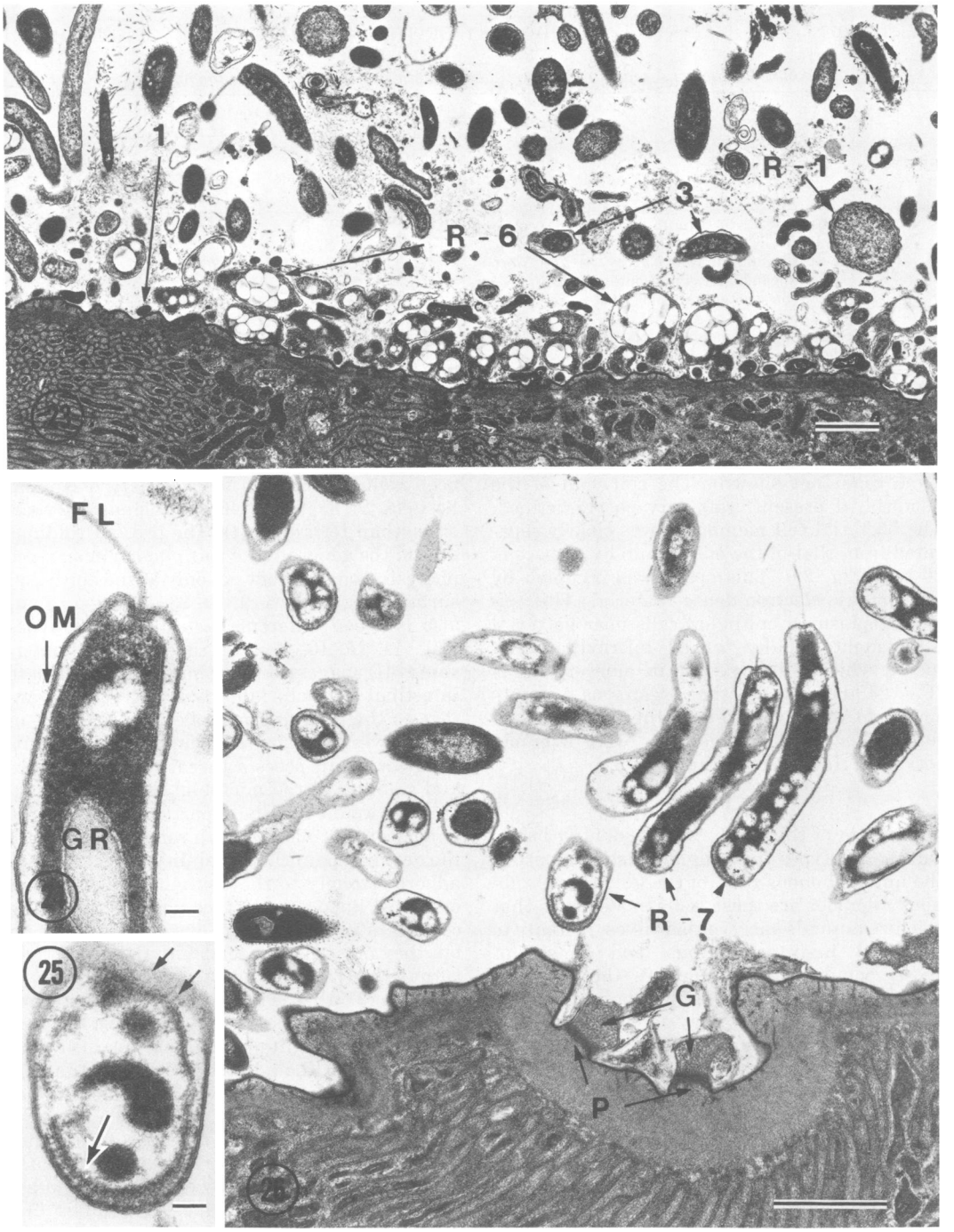

FIG. 23. *Transmission electron micrograph of the paunch epithelium and associated microbiota of an R. flavipes worker obtained from a field infestation. Note the abundance of R-6 cells, in addition to morphotype 1, 3, and R-1 cells. Bar = 1 μm.*

FIG. 24. *Longitudinal section of one end of an R-7 cell showing the single polar flagellum (FL), the outer membrane (OM), and intracytoplasmic granules (GR). Bar = 0.1 μm.*

FIG. 25. *Oblique section of the flagellum-free pole of an R-7 cell showing peglike connections (single arrow) between the outer membrane and the main protoplasmic body. Note the striations (double arrows) on the outer membrane. Bar = 0.1 μm.*

FIG. 26. *Thin section of R-7 cells near the paunch epithelium of an R. flavipes soldier collected from a natural infestation. Note the overall curved shape of R-7 and the single polar flagellum. The epithelial cup has protrusions (P) that appear to release granules (G). Bar = 1 μm.*

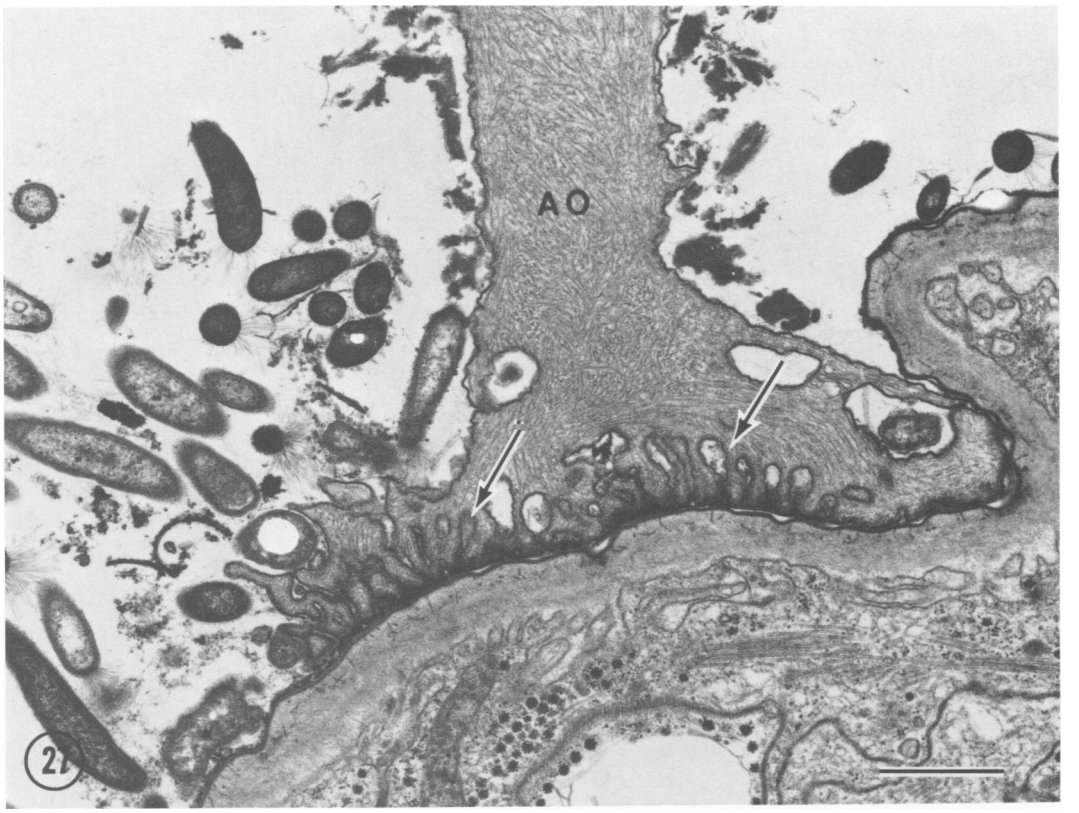

FIG. 27. *Thin section of an attachment organelle (AO) of P. vertens closely associated with the paunch epithelium of an R. flavipes worker. Numerous invaginations of the protozoan cell membrane occur at the attachment interface (arrows). Ruthenium red. Bar = 1 μm.*

shaped cells. This type of holdfast material was similar to that found on certain rod-shaped bacteria present in human gingival plaque (22).

Maintenance of termites in the laboratory imposed artificial conditions on these subterranean animals. Not only was their mobility restricted, but temperature fluctuations were far less drastic than would have occurred in their natural environment. It was not surprising, therefore, to find that the paunch microbiota of *R. flavipes* sampled directly from the field infestation was somewhat different from that of LM specimens. It appears, then, that environmental factors can alter the relative abundance of some bacterial morphotypes in the paunch. Indeed, the diet of termites has a marked effect on the nitrogen-fixing (14) and methanogenic (13) activity of the gut biota, which may reflect, in part, a change in the population levels of microbes involved in these processes. Environmental differences (e.g., the origin of termites) may explain why Bloodgood et al. (11) did not observe attachment of *Pyrsonympha* to the hindgut wall of their specimens of *R. flavipes*, whereas this was a fairly regular occurrence in ours. Furthermore, different species of termites may vary in their ability to host a dense population of bacteria on their paunch epithelium. Perhaps this is why Bloodgood (10) never found bacteria attached to the hindgut cuticle of *R. tibialis*, an observation in marked contrast to our findings with *R. flavipes* and *C. formosanus*.

One of the most intriguing features of the paunch of *R. flavipes* and *C. formosanus* were the cuplike indentations on the epithelial surface. The abundance of mitochondria near the cups, amid numerous infoldings of the cytoplasmic membrane, was an arrangement typically found in transporting epithelia (9) and suggested that cups were sites of active transport of ions. In most insects the midgut and midgut caeca are the major sites of nutrient absorption (9, 16). However, in xylophagous termites the bulk of cellulose fermentation takes place by protozoa in the paunch (24), and an enteric

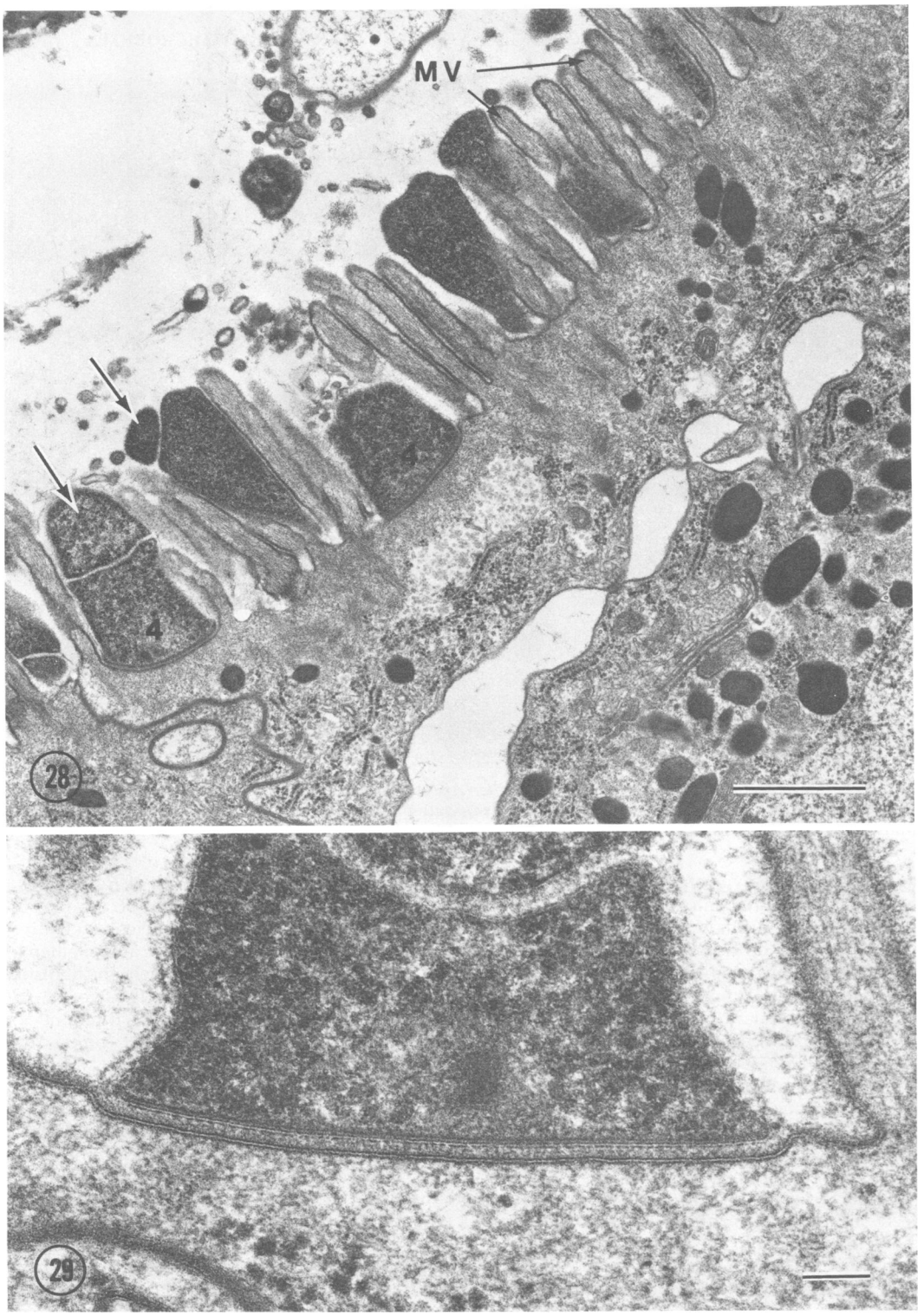

FIG. 28. *Thin section of morphotype 4 cells present among the microvilli (MV) of the midgut of an R. flavipes worker. Some of the bacteria are present as "doublets" (unlabeled arrows), which appear to remain together after cell division. Bar = 1 μm.*

FIG. 29. *High-magnification transmission electron micrograph of the cell junction between midgut epithelium and a morphotype 4 cell in an R. flavipes worker. A portion of a microvillus is included in the right side of the micrograph. Bar = 0.1 μm.*

valve prevents refluxing of paunch material back to the midgut (37). Thus, acetate, a major fermentation product of paunch protozoa (25, 26), and which serves as an energy source for termites (26), must be absorbed by the hindgut (26, 37). It is possible that the cuplike structures are specific sites for acetate (and perhaps other nutrient) absorption. Baccetti (4) observed similar cuplike structures in the paunch epithelium of the Mediterranean termite *R. lucifugus* and also considered them to be sites for nutrient absorption. To our knowledge, cups are not found in the paunch of higher (i.e., more highly evolved) termites.

The present communication represents the first detailed study of the in situ morphology of termite gut bacteria and their association with the gut epithelium. Although cellulolytic protozoa are certainly critical to the survival of xylophagous termites (13, 23, 27), it seems clear that any attempts to address the biochemical ecology of the gut microbiota or the overall importance of the microbiota to the vitality of termites cannot afford to ignore the bacteria. Not only do procaryotes represent an abundant and morphologically diverse segment of the gut population, but also many of them are intimately associated with the alimentary epithelium. Such physical intimacy with the host probably reflects an underlying biochemical mechanism(s), since the attachment of bacteria to the gut epithelium (particularly in the region of paunch epithelial cups and between midgut microvilli) should afford a prime opportunity for nutrient exchange between the cells.

ACKNOWLEDGMENTS

We are grateful to G. R. Esenther, J. W. Mertins, and H. C. Coppel for supplying us with *C. formosanus* and for valuable advice on the maintenance and manipulation of termites. We also thank M. J. Klug and R. L. Uffen for their critical reading of the manuscript. A. Ackerson skillfully assisted with the SEM.

This investigation was supported by the Agricultural Experiment Station of Michigan State University and by National Science Foundation grant BMS75-05850 awarded to J. A. Breznak.

LITERATURE CITED

1. **Akin, D. E.** 1976. Ultrastructure of rumen bacterial attachment to forage cell walls. Appl. Environ. Microbiol. 31:562-568.
2. **Alexander, M.** 1971. Microbial ecology, p. 224-246. John Wiley and Sons, Inc., New York.
3. **Anderson, T. F.** 1951. Techniques for the preservation of three dimensional structure in preparing specimens for the electron microscope. Trans. N.Y. Acad. Sci. 13:130-133.
4. **Baccetti, B.** 1963. Ricerche sull'ultrastruttura dell'intestino degli insetti. III. Il mesentero ed il colon nell'operaio di *Reticulitermes lucifugus* Rossi. Symp. Genet. Biol. Ital. 11:230-255.
5. **Ball, G. H.** 1969. Organisms living on and in protozoa, p. 565-718. *In* T-T. Chen (ed.), Research in protozoology, vol. 3. Pergamon Press, New York.
6. **Bauchop, T., R. T. J. Clarke, and J. C. Newhook.** 1975. Scanning electron microscope study of bacteria associated with the rumen epithelium of sheep. Appl. Microbiol. 30:668-675.
7. **Beckwith, T. D., and S. F. Light.** 1927. The spirals within the termite gut for class use. Science 66:656-657.
8. **Berlin, J. D., and J. C. Ramsey.** 1970. Electron microscopy of the developing cotton fiber, p. 128-129. *In* C. J. Arceneaux (ed.), 28th Proceedings of the Electron Microscopy Society of America, 1970. Claitor's Publishing Division, Baton Rouge, La.
9. **Berridge, M. J., and J. L. Oschman.** 1972. Transporting epithelia. Academic Press Inc., New York.
10. **Bloodgood, R. A.** 1975. Ultrastructure of the attachment of *Pyrsonympha* to the hind-gut wall of *Reticulitermes tibialis*. J. Insect Physiol. 21:391-399.
11. **Bloodgood, R. A., K. R. Miller, T. P. Fitzharris, and J. R. McIntosh.** 1974. The ultrastructure of *Pyrsonympha* and its associated microorganisms. J. Morphol. 143:77-106.
12. **Breznak, J. A.** 1973. Biology of nonpathogenic, host-associated spirochetes. Crit. Rev. Microbiol. 2:457-489.
13. **Breznak, J. A.** 1975. Symbiotic relationships between termites and their intestinal microbiota, p. 559-580. *In* D. H. Jennings and D. L. Lee (ed.), Symbiosis (Society for Experimental Biology Symposium Ser., no. 29). Cambridge University Press, Cambridge.
14. **Breznak, J. A., W. J. Brill, J. W. Mertins, and H. C. Coppel.** 1973. Nitrogen fixation in termites. Nature (London) 244:577-580.
15. **Brooker, B. E., and R. Fuller.** 1975. Adhesion of lactobacilli to the chicken crop epithelium. J. Ultrastruct. Res. 52:21-31.
16. **Chapman, R. F.** 1975. The insects—structure and function, p. 56-69. American Elsevier Publishing Co., Inc., New York.
17. **Cleveland, L. R., and A. V. Grimstone.** 1964. The fine structure of the flagellate *Mixotricha paradoxa* and its associated micro-organisms. Proc. R. Soc. London Ser. B 159:668-686.
18. **Costerton, J. W., J. M. Ingram, and K.-J. Cheng.** 1974. Structure and function of the cell envelope of gram-negative bacteria. Bacteriol. Rev. 38:87-110.
19. **Esenther, G. R.** 1969. Termites in Wisconsin. Ann. Entomol. Soc. Am. 62:1274-1284.
20. **Fahmy, A.** 1967. An extemporaneous lead citrate stain for electron microscopy, p. 148-149. *In* C. J. Arceneaux (ed.), 25th Proceedings of the Electron Microscopy Society of America. Claitor's Book Store, Baton Rouge, La.
21. **Foglesong, M. A., D. H. Walker, Jr., J. S. Puffer, and A. J. Markovetz.** 1975. Ultrastructural morphology of some prokaryotic microorganisms associated with the hindgut of cockroaches. J. Bacteriol. 123:336-345.
22. **Halhoul, N., and J. R. Colvin.** 1974. The novel structure of a microorganism of human gingival plaque. Can. J. Microbiol. 20:1307-1309.
23. **Honigberg, B. M.** 1970. Protozoa associated with termites and their role in digestion, p. 1-36. *In* K. Krishna and F. M. Weesner (ed.), Biology of termites, vol. 2. Academic Press Inc., New York.
24. **Hungate, R. E.** 1938. Studies on the nutrition of *Zootermopsis*. II. The relative importance of the termite and the protozoa in wood digestion. Ecology 19:1-25.
25. **Hungate, R. E.** 1939. Experiments on the nutrition of *Zootermopsis*. III. The anaerobic carbohydrate dissimilation by the intestinal protozoa. Ecology 20:230-244.
26. **Hungate, R. E.** 1943. Quantitative analysis on the cel-

lulose fermentation by termite protozoa. Ann. Entomol. Soc. Am. 36:730–739.
27. **Hungate, R. E.** 1955. Mutualistic intestinal protozoa, p. 159–199. *In* S. H. Hutner and A. Lwoff (ed.), Biochemistry and physiology of protozoa, vol. 2. Academic Press Inc., New York.
28. **King, E. G., Jr., and W. T. Spink.** 1974. Laboratory studies on the biology of the Formosan subterranean termite with primary emphasis on young colony development. Ann. Entomol. Soc. Am. 67:953–958.
29. **Koidzumi, M.** 1921. Studies on the intestinal protozoa found in the termites of Japan. Parasitology 13:235–309.
30. **Kovoor, J.** 1959. Anatomie du tractus intestinal dans le genre *Microcerotermes* (Silvestri), (Isoptera, Termitidae). Bull. Soc. Zool. Fr. 84:445–457.
31. **Kovoor, J.** 1968. L'intestin d'un Termite Supérieur (*Microcerotermes edentatus*, Wasman, Amitermitinae). Histophysiologie et flore bactérienne symbiotique. Bull. Biol. Fr. Belg. 102:45–84.
32. **Kudo, R. R.** 1966. Protozoology, 5th ed. Charles C Thomas Publishers, Springfield, Ill.
33. **Luft, J. H.** 1961. Improvements in epoxy resin methods. J. Biophys. Biochem. Cytol. 9:407–414.
34. **Nalbandian, J., M. L. Freedman, J. M. Tanzer, and S. M. Lovelace.** 1974. Ultrastructure of mutants of *Streptococcus mutans* with reference to agglutination, adhesion, and extracellular polysaccharide. Infect. Immun. 10:1170–1179.
35. **Nelson, D. P., and L. J. Mata.** 1970. Bacterial flora associated with the human gastrointestinal mucosa. Gastroenterology 58:56–61.
36. **Noirot, C., and C. Noirot-Timothée.** 1967. L'épithélium absorbant de la panse d'un Termite supérieur. Ultrastructures et rapport avec la symbiose bactérienne. Apn. Soc. Entomol. Fr. 3:577–592.
37. **Noirot, C., and C. Noirot-Timothée.** 1969. The digestive system, p. 49–88. *In* K. Krishna and F. M. Weesner (ed.), Biology of termites, vol. 1. Academic Press Inc., New York.
38. **Pate, J., and E. J. Ordal.** 1967. The fine structure of *Chondrococcus columnaris*. III. The surface layers of *Chondrococcus columnaris*. J. Cell Biol. 35:37–51.
39. **Savage, D. C.** 1970. Associations of indigenous microorganisms with gastrointestinal mucosal epithelia. Am. J. Clin. Nutr. 23:1495–1501.
40. **Savage, D. C.** 1972. Associations and physiological interactions of indigenous microorganisms and gastrointestinal epithelia. Am. J. Clin. Nutr. 25:1371–1379.
41. **Savage, D. C., and R. V. H. Blumershine.** 1974. Surface-surface associations in microbial communities populating epithelial habitats in the murine gastrointestinal ecosystem. Infect. Immun. 10:240–250.
42. **Shea, S. M.** 1971. Lanthanum staining of the surface coat of cells—its enhancement by the use of fixatives containing Alcian blue or cetylpyridinium chloride. J. Cell Biol. 51:611–620.
43. **Smith, H. E., and H. J. Arnott.** 1974. Epi- and endobiotic bacteria associated with the external surface of *Pyrsonympha vertens*, a symbiotic protozoon of the termite *Reticulitermes flavipes*. Trans. Am. Microsc. Soc. 93:180–194.
44. **Smith, H. E., H. E. Buhse, Jr., and S. J. Stamler.** 1975. Possible formation and development of spirochaete attachment sites found on the surface of symbiotic polymastigote flagellates of the termite *Reticulitermes flavipes*. Biosystems 7:374–379.
45. **Smith, H. E., S. J. Stamler, and H. E. Buhse, Jr.** 1975. A scanning electron microscope survey of the surface features of polymastigote flagellates from *Reticulitermes flavipes*. Trans. Am. Microsc. Soc. 94:401–410.
46. **Takeuchi, A., and J. A. Zeller.** 1972. Ultrastructural identification of spirochetes and flagellated microbes at the brush border of the large intestinal epithelium of the rhesus monkey. Infect. Immun. 6:1008–1018.
47. **Tannock, G. W., and D. C. Savage.** 1974. Association of microorganisms with the epithelium in the alimentary tract of *Aspicularis tetraptera*. Infect. Immun. 9:475–476.
48. **Tannock, G. W., and J. M. B. Smith.** 1970. The microflora of the pig stomach and its possible relationship to ulceration of the pars oesophagea. J. Comp. Pathol. 80:359–367.
49. **Wang, W. S., and D. G. Lundgren.** 1969. Poly-β-hydroxybutyrate in the chemolithotrophic bacterium *Ferrobacillus ferrooxidans*. J. Bacteriol. 97:947–950.
50. **Watson, M. L.** 1958. Staining of tissue sections for electron microscopy with heavy metals. J. Biophys. Biochem. Cytol. 4:475–478.